Unsteady fluid dynamics using matched asymptotics: Analysis, design and control

Shreyas Mandre

Summary: The goal of this project is to study high Reynolds number ($\sim 10^4 - 10^6$) flow optimization and control, develop a course on *Control theory using biomechanics*, and establish a long term resource to introduce Providence public school students to engineering. Nonlinear dynamics and presence of multiple scales makes optimization and control of high Reynolds number flow notoriously difficult. Engineers and scientists have limited success in understanding various phenomena in this regime; for instance the superior ability of insects, small birds and fish in their propulsive efficiency. I present an efficient computational framework based on matched asymptotic expansion of the unsteady solution of Navier-Stokes equations to determine the flow around moving rigid and flexible bodies in two and three dimensions. This method is amenable to an equally efficient computation of the adjoint variables, which makes it adaptable to advanced optimization and control routines. I propose using this method to determine the optimal strokes of objects inspired by birds, insects, and fish, and to control robotic propulsive mechanisms. For the educational component, I design an interdisciplinary undergraduate course, which uses biomechanical behavior as motivation for learning control theory. An integrated outreach component aims at constructing a robotic toolbox to be used extensively in the Providence school district to benefit underprivileged public school students, 85% of whom belong to low-income households.

Intellectual merit: Formulation of Prandtl's boundary layer, and the Kutta condition for vorticity shed by an airfoil, culminated in an elegant description of steady flow around streamlined bodies, which appears in every introductory textbook on fluid dynamics. However, the Kutta condition is not applicable to flows around smooth bodies (e.g. elliptical wings) and may not be valid in extremely unsteady situations, which are the topic of heavy investigation today. In this research, I propose the minimal reduced model for vortex shedding from smooth bodies in unsteady flow, which functions analogously to the Kutta condition and is derived from first principles. Applying this reduced model provides approximately 100-fold speedup in computation compared to other methods currently available and provides comparable accuracy. Using this model, application of optimization and control principles to aerodynamic and hydrodynamic flows becomes feasible, enabling solutions of biomechanics and robotic control problems previously not possible.

Broader impact: The results from this research will influence fields of science and engineering beyond computational fluid dynamics, including engineering design and biology. This research will enable determining how close an animal or robotic propulsive stroke is to minimizing expended energy or maximizing propulsive force. The results will also establish a basis for design of traditional and bio-mimetic robots pursued in the interest of safety and national security.

Outreach: Low-cost robotic platforms provide an ideal way to introduce school students to engineering concepts. Establishing an educational and outreach toolbox based on such platforms is bound to have an immense impact on the Providence public school students. This toolbox will be maintained by me, and used for my outreach activity to local schools. The toolbox will be shared with other members of the community for the purpose of integration in educational activity for local school students.

Education: The educational component integrates this research into an interdisciplinary undergraduate and graduate education and mentoring, training the next generation of fluid and computational scientists. The undergraduate course on *Control theory using biomechanics* uses inquiry-based teaching technique by employing computational tools for interdisciplinary education. Using this technique, principles behind a host of biomechanical behavior are treated. The educational component also integrates mentoring of undergraduate and graduate students in fields of interdisciplinary research.

Figure 1: Propulsive strokes of (a) birds and (b) insects, and (c) fish impart them with capabilities difficult to reproduce technologically.

1 Introduction

Bio-locomotion using high Reynolds number (Re) unsteady fluid dynamics is an active area of research. The ability of many birds[1], mammals[2,3], insects[4–8], fish[2,9] (depicted in figure 1) to control the unsteady flow around them currently appears to be outside the range of robotic mimics[10]. Effective manipulation and control of unsteady effects at high Reynolds numbers are considered to underlie the superior performance of these organisms. As the robotics community pushes the limits on engineering, it is useful to know the fundamental performance limits under various fluid-structure interaction settings, e.g. maximum propulsive power of a flexible fin[11–14], or the maximum lift possible from a periodically flapping wing[15–17]. The set of beneficial unsteady effects is small and hence, has proved difficult to find[18]. The challenge is to develop a reasonable strategy for scanning the large space of all possible motions and deformations of the body to determine the beneficial set. Optimization and control theory, with calculus of variations at its foundation[19], provides a framework for tackling this complexity. Steady progress on a control theoretic framework applied to steady and unsteady fluid dynamics has resulted in significant advances since the late 1980s[20–26]. In a nutshell, the strategy is to couple methods of solving the governing Navier-Stokes equations with adjoint-based gradient calculations to facilitate optimization and control. For example to find the maximum lift possible from the unsteady stroke of a wing, one can use gradient descent algorithms on the periodic flapping stroke to successively improve the stroke until a local optimum is found (analogous to procedure used by Pesavento & Wang[18]). However, the presence of nonlinearities and multiple scales in the fluid dynamics impedes rapid computation of the flow.

This proposal aims to determine principles underlying aerial and aquatic bio- and robotic locomotion by applying the framework of adjoint-based optimization to locomotive strokes using a fast method for predicting the flow resulting from the motion of a rigid or flexible solid bodies.

1.1 Approach: At large Re, vorticity is the principle dynamic quantity of interest[27]. The velocity field can be represented using the Biot-Savart law in terms of the vorticity, and so can be the forces and torques on the body. Vorticity is generated at the walls of the solid body, and is transported away from it in the boundary layer. The vorticity leaves the boundary layer at a point of flow separation and is introduced in the bulk fluid. Once outside the boundary layer, viscous diffusion of the vorticity may be neglected owing to high Re, and the vorticity dynamics are predominately governed by advection and stretching. Vortex methods can efficiently model the flow outside the boundary layer, but a simple and efficient method for modeling the generation and shedding of vorticity from the boundary layer is needed.

I present a computational framework based on matched asymptotic methods, similar to the one used by Booty & Siegel[28], for determining the strength of shed vorticity from the boundary layer. This framework leads to a O(100) fold reduction in the computation time for the flow compared to current methods, and allows an equally efficient computation of the adjoint variables. I propose to use this framework for optimization and control of high Re *bio-locomotion.*

	2D scaling	**Estimate**	**3D scaling**	**Estimate**
Reynolds number	$\mathrm{Re} = Ua/\nu$	10^4	$\mathrm{Re} = Ua/\nu$	10^4
Boundary layer thickness	$\delta = a\mathrm{Re}^{-1/2}$	$10^{-2}a$	$\delta = a\mathrm{Re}^{-1/2}$	$10^{-2}a$
Grid spacing	$h = \delta/10$	$10^{-3}a$	$h = \delta/10$	$10^{-3}a$
Number of grid points	$N_g = a^2/h^2$	10^6	$N_g = a^3/h^3$	10^9
Time step limit	$\Delta t = h/U$	$10^{-3}a/U$	$\Delta t = h/U$	$10^{-3}a/U$
Number of time steps	$N_t = 10a/U\Delta t$	10^4	$N_t = 10a/U\Delta t$	10^4
Flops per time step (Fast Poisson solver)	$N_s = 10^3 N_g \log(N_g)$	10^{10}	$N_s = 10^3 N_g \log(N_g)$	10^{12}
Flops per solution	$N_{sol} = N_s N_t$	10^{14}	$N_{sol} = N_s N_t$	10^{16}
Flops per adjoint	$N_{adj} = N_{sol} \log N_t$	10^{15}	$N_{adj} = N_{sol} \log N_t$	10^{17}
Number of iterations for optimization	N_{iter}	20	N_{iter}	20
Total flops for optimization	$N_{adj}N_{iter}$	10^{16}	$N_{adj}N_{iter}$	10^{18}
Desktop speed	R (in flops/sec)	10^{10}	R (in flops/sec)	10^{10}
Wall time per solution	$t_w = N_{sol}/R$	10^4 sec O(hours)	$t_w = N_{sol}/R$	10^6 sec O(week)
Wall time per adjoint	$t_{adj} = N_{adj}/R$	10^5 sec O(day)	$t_{adj} = N_{adj}/R$	10^7 sec O(months)
Total wall time for optimization	$t_{total} = N_{iter}t_{adj}$	O(month)	$t_{total} = N_{iter}t_{adj}$	O(years)

Table 1: An order-of-magnitude estimate of the computational complexity and expected computational wall time for the execution of stroke optimization for flow of characteristic speed U past a body of characteristic size a at a Reynolds number of 10^4. The various prefactors governing the accuracy of the solution are chosen here to reflect the best estimates from literature, but err on the side of under-estimation. Real computational time experienced by researchers is higher by upto two orders of magnitude.

1.2 Background: Numerically solving the governing Navier-Stokes equations using primitive variables is prohibitively expensive from the perspective of flow optimization and control. A simple back-of-the-envelope estimate of the computational effort for solving the flow corresponding to a Reynolds number of 10^4, shown in table 1, highlights this issue. The primary expense arises from resolving the boundary layer; its thickness dictates the number of grid points to be used for spatial discretization, and the time step through the CFL condition. On modern desktop computers one flow solution in 2D takes at least hours, and in 3D takes at least days. (The computational effort shown in table 1 is grossly underestimated; flow past stationary, moving and flexible bodies at $\mathrm{Re} \approx 10 - 10^3$ takes a few CPU-days[29] in 2D, and CPU-weeks in 3D[18,29], and very little data is available for larger Re.) Calculating the adjoint variables and implementing a gradient based optimization algorithm[24] increases the computational time to at least months for 2D problems (years for 3D). Methods like Large Eddy Simulations model sub-grid scale eddies, but still have to resolve the boundary layer to accurately predict the shed vorticity, and hence are not exempt from this estimate. Parallel computing on a cluster of processors can reduce the 2D computational time to few days and today's (June 2013) top 5 supercomputers[30] may be able to reduce the computational time for 3D to several hours, if the algorithms are effectively parallelized, but it is uncertain how data dependencies can be addressed for parallelization. In conclusion, optimization, state estimation, and control are still out of range of computational fluid dynamics.

An hierarchy of reduced order models of fluid flow provide an alternative to avoid the computational effort for the solution of Navier-Stokes equations, at the expense of reduced (or sometimes uncertain) accuracy. All these models identify that viscous effects in the flow may be neglected except for the process of vorticity shedding from the body. The simplest of these models[31–36] apply

Outer velocity: $\boldsymbol{u}_{\text{out}}^{n+1} = \tilde{\boldsymbol{u}}_I^{n+1} + \tilde{\boldsymbol{u}}_{\text{new}}^{n+1} + \boldsymbol{\nabla}\phi^{n+1}, \quad p^{n+1} = p_1 + p_2$

1. Advect vortices ($k = 1, 2, \ldots, N^n$) according to
$$\boldsymbol{r}_k^{n+1} = \boldsymbol{r}_k^n + \Delta t \left[\boldsymbol{\nabla}\phi^n(\boldsymbol{r}_k^n) + \sum_{j=1, j\neq k}^{N^n} \frac{\Gamma_j \hat{\boldsymbol{z}} \times (\boldsymbol{r}_k^n - \boldsymbol{r}_j^n)}{2\pi |\boldsymbol{r}_k^n - \boldsymbol{r}_j^n|^2} \right]$$

2. Define components of $\tilde{\boldsymbol{u}}_I^{n+1}$ at $\boldsymbol{x}$ on the interface:
$$\tilde{\boldsymbol{u}}_I^{n+1} = \sum_{j=1}^{N^n} \frac{\Gamma_j \hat{\boldsymbol{z}} \times (\boldsymbol{x} - \boldsymbol{r}_j^{n+1})}{2\pi |\boldsymbol{x} - \boldsymbol{r}_j^{n+1}|^2} \quad \equiv \quad \tilde{u}_I^{n+1} \hat{\boldsymbol{t}} + \tilde{v}_I^{n+1} \hat{\boldsymbol{n}}$$

3. Calculate p_1 at the interface:
$$\frac{\tilde{u}_I^{n+1} - (u^n - \phi_\theta^n)}{\Delta t} + u^n u_\theta^n + v^n v_\theta^n + p_{1,\theta} = 0.$$

5. Define $\dfrac{\phi_\theta^{n+1} - \phi_\theta^n}{\Delta t} + p_{2,\theta} = 0$. p_2 and ϕ^{n+1} solved in step 12.

9. Introduce new vortices outside the boundary layer to match the shed vorticity and $\tilde{\boldsymbol{u}}_{\text{new}}^{n+1} \cdot \hat{\boldsymbol{t}} = u_c^{n+1}$ from this shed vorticity. See figure 3 for details. Formally, $\tilde{\boldsymbol{u}}_{\text{new}}^{n+1}/\Delta t + \boldsymbol{u} \times \omega \hat{\boldsymbol{z}} = 0$.

11. Calculate the total normal velocity component in terms of ϕ^{n+1}:
$$\boldsymbol{u}_{\text{out}}^{n+1} \cdot \hat{\boldsymbol{n}} = \phi_\eta^{n+1} + (\tilde{\boldsymbol{u}}_I^{n+1} + \tilde{\boldsymbol{u}}_{\text{new}}^{n+1}) \cdot \hat{\boldsymbol{n}}.$$

12. Solve $\nabla^2 \phi^{n+1} = 0$ satisfying boundary condition that the normal velocities calculated in steps 10 and 11 match exactly, i.e. $\boldsymbol{u}_{\text{out}}^{n+1} \cdot \hat{\boldsymbol{n}} = v_0^{n+1} + v^{n+1}$. Update p_2 and u_b^{n+1} using ϕ^{n+1}.

Adding steps 3, 5 and 9 gives the tangential component of
$$\frac{\boldsymbol{u}_{\text{out}}^{n+1} - \boldsymbol{u}_{\text{out}}^n}{\Delta t} + \boldsymbol{u}^n \times \omega \hat{\boldsymbol{z}} + \boldsymbol{\nabla}\left(p^{n+1} + \frac{|\boldsymbol{u}_{\text{out}}^n|^2}{2} \right) = 0.$$

At $\eta = \eta_{\max}$, both components of velocity fields match exactly:
$\tilde{u}_I^{n+1} + \tilde{\boldsymbol{u}}_{\text{new}}^{n+1} \cdot \hat{\boldsymbol{t}} + \phi_\theta^{n+1} = u_a^{n+1} + u_c^{n+1} + u_b^{n+1} + q(\theta) u_h^{n+1}$ (steps 4, 6, 8 and 9) and $\boldsymbol{u}_{\text{out}}^{n+1} \cdot \hat{\boldsymbol{n}} = v_0^{n+1} + v^{n+1}$ (step 12).

Boundary layer velocity: $u^{n+1} = u_a^{n+1} + u_b^{n+1} + u_c^{n+1} + q(\theta) u_h^{n+1}$

4. Compute u_a^{n+1} satisfying ($\omega^n = u_\eta^n - v_\theta^n$)
$$\frac{u_a^{n+1} - (u^n - \phi_\theta^n)}{\Delta t} + u^n u_\theta^n + v^n u_\eta^n + p_{1,\theta} - \nu u_{a,\eta\eta}^{n+1} = [v^n \omega^n]_{\eta=\eta_{\max}}$$
$$u_a^{n+1} = u_0^{n+1} \text{ at } \eta = 0, \quad u_{a,\eta\eta}^{n+1} = 0 \text{ at } \eta = \eta_{\max}.$$
p_1 is defined (in step 3) such that at $\eta = \eta_{\max}$, $u_a^{n+1} = \tilde{u}_I^{n+1}$.

6. Define $\dfrac{u_b^{n+1} - \phi_\theta^n}{\Delta t} + p_{2,\theta} = 0$. Note that $u_b^{n+1} = \phi_\theta^{n+1}$.

7. Define $\dfrac{u_c^{n+1}}{\Delta t} = -[v^n \omega^n]_{\eta=\eta_{\max}}$, to model shed vorticity.

8. u_h^{n+1} is used to satisfy no-slip boundary condition.
$$\frac{u_h^{n+1}}{\Delta t} = \nu u_{h,\eta\eta}^{n+1} \qquad \begin{cases} u_h^{n+1} = 1 \text{ at } \eta = 0 \\ u_h^{n+1} = 0 \text{ at } \eta = \eta_{\max} \end{cases}$$
$$\Rightarrow u_h^{n+1} = \frac{\sinh(\eta_{\max} - \eta/\sqrt{\nu \Delta t})}{\sinh(\eta_{\max}/\sqrt{\nu \Delta t})}.$$
Set $q = -u_b^{n+1} - u_c^{n+1}$ so that $u^{n+1} = u_0^{n+1}$ at $\eta = 0$.

10. Calculate the normal velocity component in terms of ϕ^{n+1} using $u_\theta^{n+1} + v_\eta^{n+1} = 0$. At the interface,
$$v^{n+1} = -\int_0^{\eta_{\max}} u_{a,\theta}^{n+1} + (\phi_{\theta\theta}^{n+1} + u_{c,\theta}^{n+1})(\eta_{\max} - \sqrt{\nu \Delta t}).$$

Adding steps 4, 6, 7 and 8 gives
$$\frac{u^{n+1} - u^n}{\Delta t} + u^n u_\theta^n + v^n u_\eta^n + p_\theta^{n+1} = \nu u_{\eta\eta}^{n+1}.$$

Table 2: Operator splitting time-stepping algorithm. The velocity and pressure are split in parts as shown on the first line, and the steps 1-12 are sequentially carried out. Left column denotes operations on the outer region, and right on boundary layer variables. The equations governing each of these parts are shown in Azure and Almond color backgrounds, and the relations between the boundary layer and outer variables are highlighted in other color backgrounds. The last line summarizes the matching of the velocity components at the interface $\eta = \eta_{\max}$.

to rigid wings. They assume the flow around the wings to be quasi-steady and model the fluid dynamic force on them in terms of the instantaneous orientation, velocity and acceleration of the wing. Versions of such models that incorporate unsteadiness[37,38] are also available. The assumptions underlying these models make them unsuitable for large amplitude unsteady motion, where the flow can separate from multiple points on the body.

Models in the next level of the hierarchy also only apply to bodies with sharp edges, but model vorticity transport according to inviscid dynamics[39–46]. These models assume that vorticity is shed only from the sharp edges of the body and then evolves into a vortex sheet. The rate of the vorticity shed is chosen so as to eliminate a singularity of the flow at these sharp edges – the celebrated Kutta condition from aerodynamics. The shed vortex sheet is usually represented by an array of discrete point vortices obeying inviscid vortex dynamics or a single tightly rolled-up point vortex (governed by the Brown-Michael vortex dynamics). These methods are also very efficient. However, they do not allow for the possibility of separation at any point other than one of the sharp edges on the body. As a result, they cannot be used to model vorticity shed from a smooth body (e.g. an elliptical wing). Moreover, in practice, vorticity is not always shed from *all* sharp edges on a body, for example, the flow may not always separate from the leading edge of a wing. These methods cannot *a priori* predict the edges at which the flow separates. Because the optimal flows are suspected to correspond to a precise control of the instance vorticity shedding switches on or off from one of the edges, or of shedding from another point on the surface of body, these models appear to mis-represent or eliminate the effects underlying the enhanced unsteady performance.

The most accurate and computationally intensive methods in the hierarchy account for the vorticity in the boundary layer as vortex sheets of variable strength at or near the surface of the body. The vortex sheets are represented as arrays of point or blob vortices and function to enforce the no-slip condition[41,47–54]. These vortices transport away from the boundary by advection and diffusion, and leave the boundary layer where the flow separates, thus accurately modeling vorticity shedding. The drawback of this method is that accurate description of flow requires computational effort comparable to direct solution of Navier-Stokes equations. It is so because the distance between the point or blob vortices should be comparable to a fraction of the boundary layer thickness, and plays a role analogous to grid spacing in direct solution of Navier-Stokes equations. These methods are not reduced order models in the strict sense, because they apply for all Re and do not take advantage of the large Re of the flow.

2 Proposed computational framework

In this proposal, I present a computational method based on matched asymptotic analysis to solve fluid-structure problems. This method combines the accuracy of the direct computational solution of Navier Stokes equations, with the computational efficiency of the reduced order models. Following the usual procedure for matched asymptotic methods, the flow domain is decomposed into a boundary layer of thickness $Re^{-1/2}$ close to the solid body, where viscous effects are important, and an outer region where they are negligible (see figure 2(a)). The separation of length scales in the boundary layer naturally leads to an efficient model based on Prandtl's boundary layer equation, which explicitly and accurately accounts for generation and transport of vorticity in the boundary layer. As this vorticity flows out of the boundary layer, the method converts it to an array of point vortices as a way of matching the velocity in the boundary layer with the outer flow. The point vortices re- entering the boundary layer imparts momentum to the fluid there, thus accounting for re-attachment. The solution automatically accounts for unsteady boundary layer separation, and thereby captures the details of mechanisms such as dynamic stall, leading edge vortex shedding, and vortex recapture. The method has a fixed computational cost as a function of Reynolds number, presented in subsection 2.7.

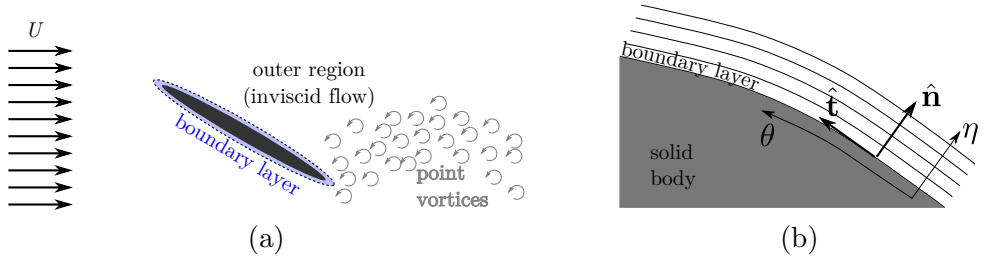

Figure 2: Schematic showing domain decomposition into an outer region and a boundary layer. (a) The flow in the outer region is described in terms of point vortices. (b) The boundary layer coordinate systems.

Below I describe a numerical approach to compute such a velocity at time step $n+1$ using the velocity at time step n (superscripts n and $n+1$ consistently denote the time step) in 2D.

2.1 Outer flow: The state of the flow at time step n in the outer region is described using an array of point vortices of strength Γ_j at location $\boldsymbol{r}_j$, $j = 1, 2, 3, \ldots, N^n$, where N^n is the number of vortices at that time step. These vortices obey inviscid dynamics, and are introduced or removed as required to match with the dynamics in the boundary layer. The fluid velocity induced by these vortices at this time step is given by

$$\boldsymbol{u}_I^n(\boldsymbol{x}) = \sum_{j=1}^{N^n} \frac{\Gamma_j \hat{\boldsymbol{z}} \times (\boldsymbol{x} - \boldsymbol{r}_j^n)}{2\pi |\boldsymbol{x} - \boldsymbol{r}_j^n|^2}. \tag{1}$$

The total fluid velocity field is $\boldsymbol{u}_{\text{out}}^n(\boldsymbol{x}) = \boldsymbol{u}_I^n(\boldsymbol{x}) + \boldsymbol{\nabla}\phi^n(\boldsymbol{x})$, where the velocity potential ϕ^n satisfying $\nabla^2\phi^n = 0$, is added to satisfy far-field boundary conditions and matching with the boundary layer. The total velocity obeys the (discretized form of) Euler equations for inviscid fluids

$$\boldsymbol{u}_{\text{out}}^{n+1} = \boldsymbol{u}_{\text{out}}^n - \Delta t \left\{ \boldsymbol{u}_{\text{out}}^n \cdot \boldsymbol{\nabla}\boldsymbol{u}_{\text{out}}^n + \boldsymbol{\nabla} p^{n+1} \right\} = \boldsymbol{u}_{\text{out}}^n - \Delta t \left\{ \boldsymbol{u}_{\text{out}}^n \times \omega \hat{\boldsymbol{z}} + \boldsymbol{\nabla} \left[p^{n+1} + \frac{|\boldsymbol{u}_{\text{out}}^n|^2}{2} \right] \right\}, \tag{2}$$

in terms of the vorticity $\omega = \hat{\boldsymbol{z}} \cdot \boldsymbol{\nabla} \times \boldsymbol{u}^n$, where the gradient of pressure p^{n+1} imposes incompressibility. From (2), momentum transport[27] is seen to arise from the $\boldsymbol{u}_{\text{out}}^n \times \omega\hat{\boldsymbol{z}}$ term, along with the gradient of the Bernoulli term. The term $\boldsymbol{u}_{\text{out}}^n \times \omega\hat{\boldsymbol{z}}$ is related to the flux of vorticity, a fact used in the matching procedure.

2.2 Boundary layer: The flow in the boundary layer is described using a body fitted coordinate system. The arc-length coordinate along the boundary layer is denoted θ and the wall normal coordinate translating normally with the body is η with the position vector $\boldsymbol{x}(\theta, \eta)$, as shown in figure 2(b). The solid body moves with velocity $\boldsymbol{u}_0(\theta) = u_0^n(\theta)\hat{\boldsymbol{t}}^n(\theta) + v_0^n(\theta)\hat{\boldsymbol{n}}^n(\theta)$, where $\hat{\boldsymbol{t}}^n$ and $\hat{\boldsymbol{n}}^n$ are unit basis vectors in the tangential and normal directions at time step n respectively. The functions u_0^n and v_0^n describe the motion of the body, which may themselves be prescribed or governed by the dynamics of the solid body. The computational method for calculating flow around rigidly moving bodies is described here; the generalization to flexible bodies needs to account for boundary layer coordinates that stretch; this detail poses no technical difficulty[28,55,56]. The fluid velocity $\boldsymbol{u}_{\text{bl}}$ is described by decomposing along the tangential and normal direction at time step n as $\boldsymbol{u}_{\text{bl}}^n(\theta, \eta) = u^n(\theta, \eta)\hat{\boldsymbol{t}}(\theta) + v^n(\theta, \eta)\hat{\boldsymbol{n}}(\theta)$. The radius of curvature of the boundary is assumed to be much larger than the boundary layer thickness, which leads to the simplified governing equations (the effect of leading order body curvature may be included without much difficulty in this formulation)

$$u_t + uu_\theta + vu_\eta + p_\theta = \nu u_{\eta\eta}, \quad p_\eta = 0, \quad u_\theta + v_\eta = 0, \tag{3}$$

where $\nu = \text{Re}^{-1}$, and subscripts denote partial derivatives. The velocity components satisfy $u = u_0$ and $v = 0$ at the solid wall $\eta = 0$. Asymptotic matching with the outer region is imposed as $\eta \to \infty$.

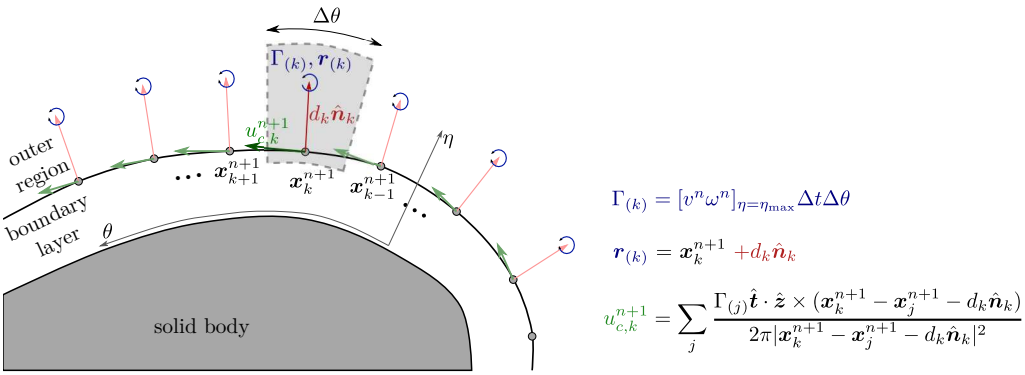

Figure 3: A schematic describing the vortex shedding method in step 9 of table 2. The vorticity flowing out of the boundary layer at point $\boldsymbol{x}_k$ with flux $v\omega$ in time Δt through each element is converted to a point vortex of strength $\Gamma_{(k)}$ (top equation). These point vortices are placed along a curve just outside the boundary layer to simulate a vortex sheet shed from the boundary layer. The position of these point vortices $\boldsymbol{r}_{(k)}$ is determined by the distance d_k outside the boundary layer (middle equation). The distances d_k are chosen so that these vortices induce tangential velocity exactly equal to the change in the boundary layer velocity component u_c^{n+1} resulting from vorticity transport to the outer region (step 7 in table 2).

Matching of normal stress implies that pressure in the boundary layer is equal to the pressure in the outer region, whereas tangential stress leads to the shedding of vorticity as shown in §2.3. Vorticity $\omega = u_\eta^n - v_\theta^n$ in the boundary layer is approximated as $\omega \approx u_\eta$ and its flux in the normal direction is $v\omega - \nu\omega_\eta \approx vu_\eta - \nu u_{\eta\eta}$. A natural boundary condition to use is that the diffusive flux of vorticity be zero so that matching with the outer inviscid flow is possible, i.e. $u_{\eta\eta} = 0$ at $\eta = \eta_{\max}$.

The boundary layer equation is discretized in time as

$$u^{n+1} - u^n + \Delta t\left(u^n u_\theta^n + v^n u_\eta^n + p_\theta^{n+1} - \nu u_{\eta\eta}^{n+1}\right) = 0, \quad p_\eta^{n+1} = 0, \quad u_\theta^{n+1} + v_\eta^{n+1} = 0. \tag{4}$$

The viscous term being the stiffest term is treated implicitly for stability, and the implicit treatment of the pressure term is related to the outer pressure p^{n+1}. The advection terms are discretized spatially using upwind differences and the viscous term is treated using central difference; the precise form of this discretization is chosen so that matching is carried out to numerical precision.

2.3 Matching: Assuming that the two flows agree exactly at the interface (between the outer region and the boundary layer) at time step n, i.e. $\boldsymbol{u}_{\text{out}}^n(\boldsymbol{x}(\theta,\eta_{\max})) = \boldsymbol{u}_{\text{bl}}^n(\theta,\eta_{\max}) = u^n\hat{\boldsymbol{t}} + v^n\hat{\boldsymbol{n}}$, the exact numerical matching at time step $n+1$ requires careful analysis of the corresponding terms in the equations governing the flow in both regions. The main difficulty is the consistent determination of the unknown pressure p^{n+1} to substitute in (4), because it depends on the outer velocity $n+1$, which in turn depends on the normal velocity in the boundary layer. However, this difficulty is solvable using a operator splitting technique presented in table 2. Using this technique, the time stepping results in a numerically exact agreement between the outer and inner flow, and can be implemented using efficient computational techniques.

The outer velocity at time step $n+1$ is split as $\boldsymbol{u}_{\text{out}}^{n+1} = \tilde{\boldsymbol{u}}_I^{n+1} + \tilde{\boldsymbol{u}}_{\text{new}}^{n+1} + \boldsymbol{\nabla}\phi^{n+1}$, where $\tilde{\boldsymbol{u}}_I^{n+1}$ is the velocity induced by the N^n vortices from time step n (now moved to their new location), $\tilde{\boldsymbol{u}}_{\text{new}}^{n+1}$ is the velocity induced by the new vortices, and $\boldsymbol{\nabla}\phi^{n+1}$ is the potential flow part.

The unknown tangential boundary layer velocity at time step $n+1$ is also decomposed as $u^{n+1} = u_a^{n+1} + u_b^{n+1} + u_c^{n+1} + q(\theta)u_h^{n+1}$, with each part playing a specific role in matching.

Matching works by requiring that each part of the outer and boundary layer (see steps 2-9 coded by backgound color in table 2) velocity decomposition satisfy an update equation so that (i) the sum of these update equations gives (2) and (4) respectively, and (ii) at the matching interface

	2D scaling	Estimate	3D scaling	Estimate
Normal grid points	N_η	50	N_η	50
Tangential grid points	N_θ	200	N_θ, N_ξ	$200, 1000$
Number of grid points	$N_g = N_\eta N_\theta$	10^4	$N_g = N_\eta N_\theta N_\xi$	10^7
Time step limit	$\Delta t = a/UN_\theta$	$5 \cdot 10^{-3} a/U$	$\Delta t = a/UN_\theta$	$5 \cdot 10^{-3} a/U$
Number of time steps	$N_t = 10a/U\Delta t$	2×10^3	$N_t = 10a/U\Delta t$	2×10^3
New vortices per time step	$\dot{N}_\Gamma = N_\theta/10$	20	$\dot{N}_\Gamma = N_\theta N_\xi/10$	2×10^4
Total number of vortices	$N_\Gamma = \dot{N}_\Gamma N_t$	4×10^4	$N_\Gamma = \dot{N}_\Gamma N_t$	4×10^7
Flops per time step				
(Boundary layer update)	$N_{bl} = 10^2 N_g$	10^6	$N_{bl} = 10^2 N_g$	10^9
(Vortex position update)	$N_v = 10^3 N_\Gamma \log(N_\Gamma)$	4×10^8	$N_v = 10^3 N_\Gamma \log(N_\Gamma)$	8×10^{11}
(Potential flow update)	$N_p = 10^2 N_\theta \log N_\theta$	2×10^5	$N_p = 10^2 N_\theta N_\xi \log(N_\theta N_\xi)$	2×10^8
Total	$N_s = \max(N_{bl}, N_v, N_p)$	4×10^8	$N_s = \max(N_{bl}, N_v, N_p)$	8×10^{11}
Flops per solution	$N_{sol} = N_s N_t$	8×10^{11}	$N_{sol} = N_s N_t$	1.6×10^{15}
Flops per adjoint	$N_{adj} = N_{sol} \log N_t$	8×10^{12}	$N_{adj} = N_{sol} \log N_t$	1.6×10^{16}
Number of iterations for optimization	N_{iter}	20	N_{iter}	20
Total flops for optimization	$N_{adj} N_{iter}$	1.6×10^{14}	$N_{adj} N_{iter}$	3.2×10^{17}
Desktop speed	R (in flops/sec)	10^{10}	R (in flops/sec)	10^{10}
Wall time per solution	$t_w = N_{sol}/R$	80 sec O(mins)	$t_w = N_{sol}/R$	1.6×10^4 sec O(hours)
Wall time per adjoint	$t_{adj} = N_{adj}/R$	800 sec O(hour)	$t_{adj} = N_{adj}/R$	1.5×10^5 sec O(day)
Total wall time for optimization	$t_{total} = N_{iter} t_{adj}$	O(day)	$t_{total} = N_{iter} t_{adj}$	O(month)

Table 3: An order-of-magnitude estimate of the computational complexity and expected computational wall time for the execution of stroke optimization using the proposed method. The computational effort is independent of Re.

each part of outer flow matches with a part of the boundary layer (see equations in steps 4, 6, 8, 9 and 12 in table 2 coded by background color). For complete details see table 2.

2.4 Forces on the body: The force $\boldsymbol{F}$, torque τ on the body and the average power P in this time step can now be found by integrating the traction $\boldsymbol{f} = -p\hat{\boldsymbol{n}} + \nu u_\eta \hat{\boldsymbol{t}}$:

$$\boldsymbol{F} = \int \boldsymbol{f}\, d\theta, \quad \tau = \int \boldsymbol{r} \times \boldsymbol{f}\, d\theta, \quad P = \int \boldsymbol{f} \cdot \boldsymbol{u}\, d\theta. \tag{5}$$

2.5 Preliminary results – impulsively started flow past a cylinder: To test the method, my group has applied it to impulsively started flow past a cylinder. A cylinder of unit radius is subject to a flow, which starts at $t = 0$ from zero to a unit uniform farfield velocity with $\mathrm{Re} = 3000$. The resulting flow is depicted in figure 4. We have verified that our results match the asymptotic[57] skin-friction and form drag for small t, and the drag coefficient and vorticity profiles[58] for large t. The vorticity field is compared with the the results of Koumoutsakos and Leonard[58] in figure 4.

2.6 Adjoint based optimization algorithms: The matching framework described in §2.3 and the procedure in table 2 is designed with optimization and control algorithms in mind. We have verified that each step described in table 2 has a corresponding adjoint variable, which is easy to identify and efficient to compute, but we have not implemented the adjoint computation.

2.7 Computational complexity: The computational effort, estimated in table 3, for our method is significantly lower than direct numerical solution of Navier-Stokes equations, because only the boundary layer region needs to be discretized. The number of grid points in the boundary layer region is independent of Re because both the boundary layer thickness and grid spacing scale as $\mathrm{Re}^{-1/2}$. The number of vortices shed per time step is a small fraction of grid points in the tangential direction because vorticity is shed only close to the outflow stagnation point. Most of the computational steps are broken down into computations that take either $\mathrm{O}(N)$ or $\mathrm{O}(N \log N)$ effort. Moreover, many procedures in the time-stepping are embarrassingly parallelizable so that extension to multiprocessor, multicore, or graphical processor unit architectures should be beneficial.

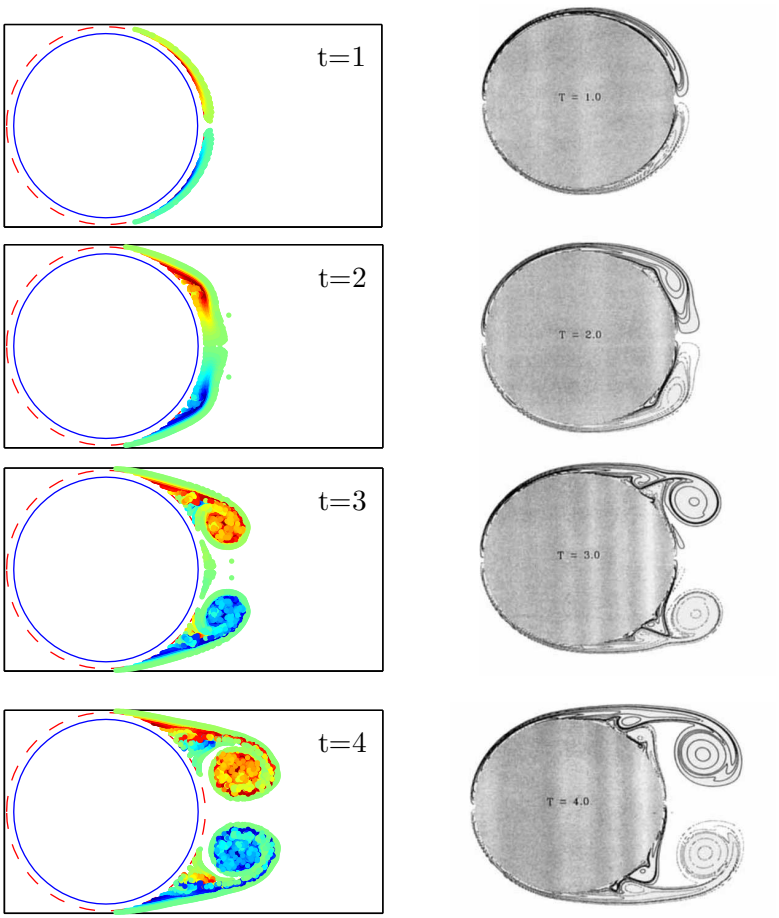

Figure 4: Vorticity shed in an impulsively started flow around a cylinder at Re = 3000. (Left) The boundary layer equations (3) are solved in a region of thickness $5\mathrm{Re}^{-1/2}$ around the cylinder, shown by the region between the red dashed line and the blue solid line. The point vortices shed from the boundary layer are color coded according to strength. The convective scale is used to non-dimensionalize time. (Right) Comparison with vorticity contour computed by Koumoutsakos and Leonard[58] (figure 21 therein).

Our method on an Apple notebook computer executes in about 10 mins for the results described in §2.5 and figure 4. This is already more than 10 times faster than traditional computational fluid dynamics at similar Re. The discrepancy between the estimate 80 s and actual execution time is traced to the direct evaluation of the sum in (1) costing us $\mathrm{O}(N_\Gamma^2)$ effort. This can be easily improved by using a fast multipole method[59,60]. We have not yet implemented the method in 3D, nor have we implemented the adjoint or the optimization schemes, and hence the 3D computational effort is only an estimate. We do, however, expect to see about 100 fold acceleration compared to direct solution of Navier-Stokes equations (similar to observations of Booty and Siegel[28]).

2.8 Remarks and limitations: Our method accounts for the different ways vorticity can be shed from the body. Any further simplification of the method results in the neglect of one or more effects, which are asymptotically not negligible, and is therefore likely to misrepresent the physics.

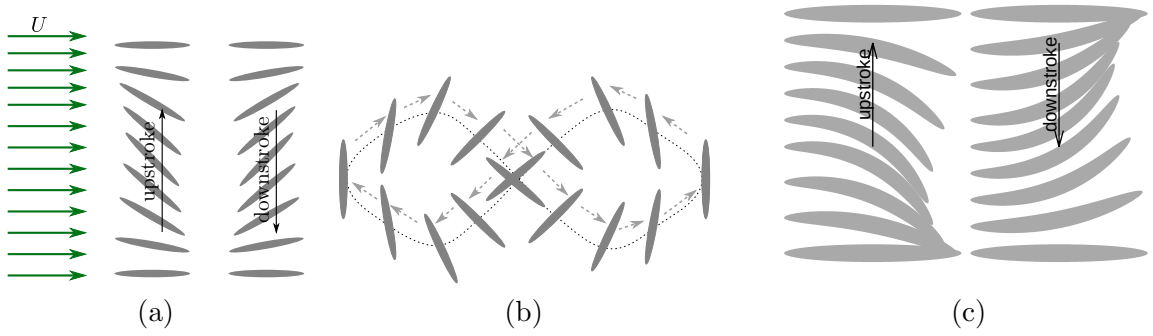

Figure 5: Examples of periodic strokes of rigid and flexible streamlined 2D bodies. (a) A two degree of freedom pitch and heave motion of a rigid body. (b) A figure 8 motion utilizing all three degrees of freedom of a rigid body. (c) Wagging motion of a flexible body similar to the sub-carangiform swimming stroke of fish.

Thus, our method represents the minimal but complete reduced order model for unsteady vortex shedding from smooth bodies.

Unlike the direct numerical solution of the Navier-Stokes equations and the vortex methods, our method has employed heuristics that makes our solution slightly different from that of the Navier-Stokes equations. In particular, we have neglected the tangential gradients of velocity in the viscous term in the boundary layer, which may not be negligible near points of flow separation (see triple-deck theories[61]). Therefore, the solution is uniformly valid everywhere except in a small region close to the point of separation. However, determining the rate of shed vorticity does not necessitate resolution of this small region. We accurately model the vorticity generated away from the separation point. Similar to the Navier-Stokes equations, the boundary layer approximation conserves vorticity. Very little vorticity accumulates in the small region near separation point, because of its small size. *Hence the vorticity shed by our scheme is expected to match the vorticity shed calculated using a direct solution of Navier-Stokes equations. Just like the Kutta condition does not resolve the flow near the trailing edge of an airfoil but predicts the vorticity shed from heuristic principle, our scheme also does the same but with greater fidelity to the Navier-Stokes equations. Thus, our scheme may be considered as a generalization of the Kutta condition for smooth bodies undergoing unsteady motion.*

What if our scheme fails in a subtle unforeseen way? Our plans may fail if actual computational effort is worse than the computational scaling presented in table 1 for problems of interest. We have planned to use the most efficient numerical methods for the solution in both the boundary layer and the outer region, but will continue to seek more efficient methods. We also plan to implement the method on parallel architecture (see step 1 on page 10). It is also not clear whether bodies with sharp leading and/or trailing edges are better suited for flow control than bodies with smooth surfaces. The current formulation of our method is for bodies with smooth surface, but it can be extended to include sharp edges using the background developed for triple deck theories[61].

3 Proposed research

My long term goal (∼10 years) is to enable real-time estimation and control of the flow around a 3D deformable body to determine best possible performance (thrust, lift, energy) for periodic (wing beat, body stroke) and transitional (startup, braking, turns) motion. The optimization problems I describe in this proposal provide a path over the next 5 years towards the long term goal.

3.1 Optimization variables and objectives: The interaction between the fluid and the solid in our mathematical model occurs through a prescription of the motion of the body. Optimization

variables for rigid bodies are easiest to describe; they are the trajectories of the bodies in the degrees of freedom of motion of the body. Sample periodic trajectories are shown in figure 5(a) and (b). For flexible bodies, the boundary of the body moves according to a combination of translation, rotation, and a deformation. An example of such a deformation mimicking a sub-carangiform swimming stroke is shown in figure 5(c). However, not every possible deformation of the boundary is physically or biologically relevant; e.g. any deformation that increases the volume of the body (area in 2D) is probably not relevant. Hence, the strokes of a flexible body need to be limited to a physically or biologically relevant set. Such a set is derived from considerations of tissue deformation in biological systems, or from principles of elasticity in engineering systems.

For a fixed free-stream fluid speed, the propulsive thrust, the lift, the work done by the fluid, and relative combinations of these quantities constitute the objective to be optimized. Some optimization problem can only be constructed for a relative quantity. Clearly, more propulsive force can always be generated by flapping the wings harder and faster, but the work done by the propulsive force cannot exceed the net work done by the motion of the solid body. Hence the objective function to maximize the propulsive force $\boldsymbol{F}$ may be written as $\mathcal{L} = \boldsymbol{F} \cdot \boldsymbol{U}/\overline{P}$, called the Froude efficiency, where $\overline{P}$ denotes the time average of the power rate over a periodic stroke, and $\boldsymbol{U}$ is the free stream velocity. Generating lift in hovering flight has a zero free stream velocity, but it has a characteristic velocity scale $U = \sqrt{W/\rho a^2}$ derived from the supported weight W, the fluid density ρ and the characteristic body size a. The optimization variable for this case is $\mathcal{L} = WU/\overline{P}$. The work done by the flow $\overline{P}$ can be optimized unconstrained, or subject to a fixed time-averaged drag.

3.2 Proposed steps: Support for 5 student-years is requested through the CAREER grant.

Step 1. (1 year) Continue accelerating the 2D computational method by implementing the vortex dynamics using fast multipole methods, as well as by converting our MATLAB code to C or Fortran 95. Parallelizing on multi-core processor and general purpose graphical processing units will also be pursued in the interest of reducing the computational time per solution, thereby opening the possibility of real-time experimental control to be implemented. This effort will inform us of the benefits and limitations of our method and the hurdles in its implementation in 3D. Distributed computing on network of computers will also be considered. This step will be implemented by a doctoral student. This exercise provides an ideal venue for undergraduate computer science students to participate in this research.

Step 2. (1 year) Formulate and implement solution of the adjoint variables. These adjoint variables are related to the adjoint variables of the Navier-Stokes equations. Because the asymptotic approximations are made before the determination of the adjoint, appropriate representations of the adjoint variables for efficient computation are automatically found. The formulation of the adjoint is a problem with appropriate complexity to engage a high-school teacher interested in research. The numerical solution of the adjoint will be carried out by a doctoral student.

Step 3. (1 year) Formulate and solve the 2D optimization problems for motion of rigid bodies. The objective function is described in §3.1. The adjoint calculated in step 2 is used in off-the-shelf optimization algorithms (steepest descent, BFGS, etc. from Numerical Recipes) and will provide important results for flow optimization for bio-locomotion and engineering. The 2D optimization will be carried out by a doctoral student.

Step 4. (1 year) Develop a 3D computational method. The effort involves implementing the vortex method in 3D, where the point vortices are replaced by curved vortex lines. The lessons learned from step 1 will be invaluable in this step. We anticipate the matching framework to be identical to one in 2D shown in table 2, except for the vector nature of velocity. The solution of boundary layer equations and the boundary element method for the velocity potential is easily generalized. The vortex shedding step shown in figure 3 will need to be extended so it becomes

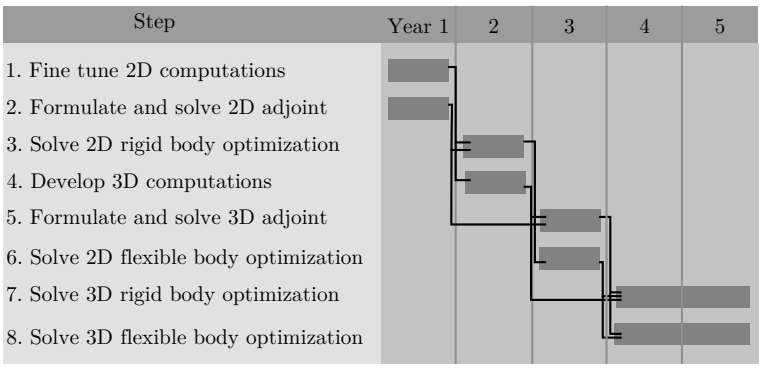

Figure 6: Gantt chart for the proposed project.

possible to find an array of vortex lines which can *exactly* match the velocity component u_c^{n+1} in the boundary layer. This step will be carried out by a doctoral student.

Step 5. (1 year) Formulate and solve 2D optimization problems for flexible bodies. The effort is to formulate the flow and adjoint problems in a boundary layer which is stretching or contracting in the tangential direction. Flexibility also introduces a non-dimensional parameter (the elasticity of the body compared to fluid forces). Investigate the dependence of the performance optimum found in step 3 as a function of this parameter. Determining and mathematically representing the set of allowable strokes by examining biologically employed actuation strategies is appropriate for an undergraduate summer project, which can be carried out in a previous year.

3.3 Concurrent and future research: The concurrent and future research plan is outlined here to provide the reviewer an idea of the long term research vision. Essentially, the 3D generalizations of the 2D problems described in §3.2 are the next logical steps towards my goal. A Gantt chart for the dependency of the steps on each other, shown in figure 6, demonstrates the feasibility of the project in 5 years, if sufficient resources (2 graduate students) are allocated. The corresponding problems of flow estimation and control are closely related to the problems described in this proposal, which also become feasible once the adjoint can be computed sufficiently rapidly. Additional funding is actively sought from other sources.

3.4 Research qualifications: I am active in developing new theoretical and computational methods for solving problems arising in physics, engineering, and biology. As an example, I constructed an asymptotic mathematical model for studying the early dynamics of droplets splashing on dry solid surfaces[62–64], which included developing suitable numerical methods to elucidate the underlying physics. I have developed and used computational methods for optimization and optimal control problems motivated by microfluidics[65] and biomechanics[66]. Both these problems used numerically computed adjoint variables. I have also published research on theoretical fluid structure interaction at both high and low Reynolds numbers[67]. I have supervised the research of student and postodoctoral collaborators at Harvard. As a faculty member at Brown, I have supervised research on the calculating the capillary force between floating objects[68], which involved numerical solution of a linear PDE using a boundary integral method. I am currently advising five graduate and one undergraduate students and have supervised two postdoctoral researchers and two undergraduate students at Brown. Thus, I am well prepared to conduct this research.

3.5 Experimental collaboration: Experimental comparison is planned through collaboration with leading experimentalist in the field (Prof. George Lauder, Department of Organismic and Evolutionary Biology, Harvard University, and Prof. Kenneth Breuer, School of Engineering, Brown University, see supporting letters) to confirm or refute our results.

4 Education and outreach

4.1 Teaching technique: I consider effective education and outreach to be integral part of my function as a faculty at Brown University. Prof. Walter Noll's opinion[69] resonate with mine, when he equates a professor to be a bridge between his research and teaching personalities. In my 7 years of teaching experience, I have participated in teaching courses on *Ordinary and Partial Differential Equations* and *Introduction to Fluid Dynamics and Transport Processes* at Harvard University as a Lecturer in Applied Mathematics, and have taught *Heat and Mass Transfer* at Brown University as an Assistant Professor. At the graduate level, I have taught *Practical Scientific Computing* and participated in teaching *Fluid Dynamics* at Harvard, and have taught *Interfacial Phenomena* and *Asymptotic and Perturbation Methods* at Brown. I have received excellent reviews, and the *Certificate of Distinction in Teaching* twice in a row at Harvard.

I have developed a technique for helping develop student intuition using computations. At the beginning of a topic in the course, I introduce and familiarize the students to a small computer program capable of simulating moderately complex phenomena, frequently inspired from current research. The program extensively uses computer visualization to represent the computed solution with physically intuitive rendering. Many students take an immediate liking to the computer program and start experimenting. Their experiments provide me with a forum to discuss and understand their observations, and thus start to build their intuition on the topic. My students, co-instructors and I have enjoyed this inquiry-based teaching technique.

4.2 Course development: At Brown University, I have developed graduate courses on *Asymptotic and Perturbation Methods* and *Interfacial Phenomena*. Many details of the matched asymptotics for high-Re flow were resolved while I was teaching the *Asymptotic and Perturbation Methods* course. This course is designed for advanced graduate students and is attended by students from physics, engineering, applied mathematics and geology. I cover traditional topics like singular perturbations, multiple scales, asymptotic approximation for integrals, and modern topics like renormalization group, using a physical and intuitive approach. A graduate student from physics, who took this course, is assisting me with the computational method. I have extensively used numerical solutions to demonstrate various concepts in this course. Next year, I plan to even better integrate computations and analysis in this course.

For the CAREER proposal, I plan to introduce an interdisciplinary undergraduate course on *Control theory using biomechanics*. The Brown curriculum prepares students in all branches of engineering with core courses on statics, dynamics, fluid and solid mechanics, etc. but lacks a course on control theory on any level. Inclusion of the proposed course in the core engineering curriculum automatically demands an interdisciplinary treatment, as well as integrates modern principles of control theory. The course will use biomechanical behavior to discuss concepts from control theory. For example, the bipedal standing of humans motivates the problem of balancing a pendulum upside down, and the gliding behavior of birds[70] motivates a discussion of aircraft flight control. Such a course allows me to integrate my research on foot biomechanics and on high-Re fluid dynamics, and provides the students the benefit of my inter-disciplinary expertise. I will actively seek feedback from students, faculty colleagues, and the Sheridan Center for Teaching and Learning at Brown, to improve the course.

4.3 Mentoring: I have participated in mentoring since 2004, when I was a graduate student at The University of British Columbia. My first experience was to guide the research of fellow graduate students under the supervision of my doctoral advisor, which led to a publication[71]. During my postdoctoral position at Harvard, I continued mentoring masters and doctoral graduate students, and also participated in mentoring fellow postdoctoral researchers leading to publications mentioned in §3.4. At Brown, I have advised the senior thesis of 2 undergraduates, and will advise

the senior thesis of another undergraduate, Khoi Nguyen, who has already published research[68] he has conducted with me. Two of the undergraduates working with me, including Khoi, were funded by the Undergraduate Teaching and Research Assistantship (UTRA) program at Brown. One of the two, Karine Ip, also won one of two Doris M. and Norman T. Halpin Prize for Interdisciplinary Senior Capstone Projects awarded in 2011-2012 for her project with me. I have mentored one woman postdoc, am currently advising 2 women graduate students (1 hispanic).

This project provides an ideal setting for mentoring an undergraduate student as a researcher. Brown funds the student for such activity through the summer UTRA program; I have advised two such projects in my three summers here. I have found that pairing an undergraduate with a graduate student or a postdoctoral researcher is an effective strategy. The pairing allows both for a closer supervision of the undergraduate students activities and the graduate student to develop mentoring skills. Meetings with the undergraduate student on a regular basis in formal and informal settings is absolutely essential in my mentoring scheme. The student also participates in regular group activity, such as group meetings and topical seminars. I also encourage the undergraduate students to participate in scientific conferences. Both Karine and Khoi have presented posters with me at the Annual APS DFD meetings[72,73], and most likely Khoi will also present a talk this year. Assistance in converting rapidly prototyped MATLAB programs into C or Fortran 95, and implementation on multiple cores or graphical processors is an ideal entry point for the undergraduates at Brown to participate in this research. Determining the set of feasible fish swimming strokes (step 5 on page 11) also provides opportunity for a biology student to participate.

Training graduate students is an integral part of this project. The topics described in this proposal are expected to fuel 2-3 doctoral theses, and nucleate ideas for many more. I encourage my graduate advisees to be interdisciplinary and explore depth as well as breadth in their research topics. My group currently investigates a wide range of problems from biomechanics, numerical methods, fluid-structure interaction, capillary phenomena, and energy harvesting. Exposure to such diverse research topics plays a crucial role in their development as scientists. All my mentees have been infected by my excitement towards science, engineering, and math, and it has inspired them to be interested in a broad range of problems. I encourage them to interact with undergraduate students and participate in mentoring. In order to develop communication skills, I insist that my advisees prepare and present at the group meeting periodically, and give at least one public talk at a national conference per year (the budget includes travel expenses for this purpose). I also manage a small lab, and I encourage all my mentees to get their hands wet by participating in experiments. This activity gives them a better understanding of the complexity of their own research and appreciation of the abilities of their experimentalist colleagues. An example of an experiment conducted in my lab can be found in a recent paper[68].

4.4 Outreach activities: The goal of the outreach activities is to establish a long-term mechanism for providing under-privileged public school students in Providence with a continuous exposure to engineering. Of the 23872 Providence public school students in 2012-2013, 15234 are Hispanic, 4335 are African American, 2105 are White, and the rest of Asian and Native American. Providence has the 3rd highest child poverty rate in America. About 85% of the public school students live in low-income households. The statistics are staggering[74]. The mechanism for this outreach activity is provided by Brown University's GK12 program managed by Prof. Karen Haberstroh, and through the AfterZone and Hub programs managed by Providence After School Alliance.

Amongst other activities, Prof. Haberstroh organizes a "scientific conference" at the local Vartan Gregorian Elementary School for 3rd to 5th grade students to expose the students to an simulated scientific conference environment (including name-tags and conference programs). The students attend a plenary lecture and presentations given by Brown University faculty.

Previous outreach: Effective outreach involves the use of captivating visuals for introduction, hands-on learning activity[75,76], and a facilitated discussion of the results[77]. I have learned to employ these elements in my outreach activity. This year, I presented a talk at the Vartan Gregorian Conference on "Tricks using surface tension", where the students carried out experiments to make metal paper clips float on the surface of water. The ensuing discussion led to an analogy of the liquid surface with a trampoline. Internet videos of water striders jumping and landing on the surface of water drove this analogy home. I feel that this year's presentation made a better impact on the students than the one I made 2 years ago in a talk entitled "Rain drops dance, fast but gracefully", which included high-speed videos of droplets but no hands-on activity.

The Vartan Gregorian students are also invited to tour the labs of Brown University once a year, giving them an inside look and familiarity with the research space. My lab regularly participates in this activity, and my lab members enthusiastically prepare and present an entertaining and educational lab tour. In previous years, we presented a soap film tunnel with a mimic of waving grass and capillary attraction between floating breakfast cereal. The year before, an undergraduate student working with me had constructed a demonstration of Faraday waves on water and cornstarch suspension, which was equally popular.

CAREER outreach: I plan to establish a flexible, easy-to-use, extensible outreach toolbox for hands-on engineering experience using robotics. The toolbox is based on the inexpensive and popular robotics and automation platforms like the LEGO MindStorms and the Arduino, and can be adapted to cater to grades 3-12. The toolbox consists of basic structural, mechanical, electrical, and electronic elements in robotics. Workshops and demonstrations can be rapidly designed and carried out using this toolbox. The toolbox is designed to be extensible, so that resources can be pooled to maintain and expand the toolbox. The toolbox will be shared with other members of the community for use in their educational and outreach activity. Such a use of robotics for outreach is found to be effective[78–80], but has not been conducted in Providence. I have allocated some funds in the budget for the acquisition of this outreach toolbox.

I plan to use such a toolbox for my conference talk and lab visit with the Vartan Gregorian students. Hands-on activity using robotic swimmers constructed using this toolbox can be effectively integrated with presentations on the topic of swimming, e.g. competitions of student-controlled robotic swimmers racing against one another. The Hub and the AfterZone programs provide a central connection for educational programs for middle- and high-school-aged students in the Providence school district organized by different institutions. Students from Brown and elsewhere, and school teachers enthusiastically organize summer-long courses, but are significantly short of resources. Ensured availability of this toolbox every summer will encourage this community of students and teacher, and many more, to design and operate programs with long term goals. One such goal is to provide the students continued exposure to robotics and to track the progress of interested students through out their school life. With these programs, I plan to develop a summer course on swimming robotics. The robotic toolbox will be an invaluable resource in Providence. Feedback on the use of the toolbox collected from the users will direct future expansion.

I plan to engage a mathematics teacher in the calculation of the adjoint for 2D problem (see step 2 on page 10), and also for the corresponding 3D problem. The effect of research participation is believed to bias the teachers towards inquiry-based teaching[81,82], a mode recommended by the American Association for Advancement of Science[83] and the National Research Council[84]. An understanding of an adjoint requires background in linear algebra, and in the context of optimization and control, calculus of variations. This calculation allows the teacher to apply her skills to a problem of practical significance. The formulation of the adjoint in 2D and 3D each can lead to a short publication, thereby assisting the teacher in her/his career. Funding to support the teacher will be sought through the NSF Research Experience for Teachers program.

5 Merit criteria

5.1 Intellectual merit: Introduction of the boundary layer by Prandtl, and the shed vorticity by Kutta, culminated in an elegant description of steady flow around streamlined bodies, which appears in every introductory textbook on fluid dynamics. However, the Kutta condition is not applicable to flows around smooth bodies (e.g. elliptical wings) and may not be valid in extremely unsteady situations, which are the topic of heavy investigation today. Similarly, flow optimization and control have been attempted for more than 50 years, in the case of aerodynamics starting with Lighthill's seminal work[85] on designing an airfoil shape to match a desired tangential velocity profile. Today this topic is also pursued actively, but major obstacles in the attempt remain to be the identification of a simple model to faithfully reproduce the fluid dynamics. In this research, I propose the minimal reduced model for vortex shedding from smooth bodies in unsteady flow, which functions analogously to the Kutta condition but is derived from first principles. Applying this reduced model provides approximately 100-fold speedup in computation compared to other currently available methods and provides comparable accuracy. Using this model, application of optimization and control principles to aerodynamic and hydrodynamic flows becomes possible, enabling solutions of biomechanics problems previously not possible.

Bio-locomotion: The fundamental mechanisms underlying superior performance of birds, insects, and fish is still an unsolved problem. The relation between morphological form and function, and the evolution of this form with time has been the centerpiece of biological investigation. Our analysis provides a detailed quantitative way of comparing the best possible performance of different morphologies.

Bio-inspiration: Engineers have been inspired by various animals in their quest for more agile, efficient and capable locomotive mechanisms. The various aquatic and aerial bio-robots need knowledge of the optimal stroke to benefit the most from the fluid dynamics. Similarly, they need a fast computational model to be able to estimate and control their trajectory. This project will realize the former in 5 years and pave a path for the latter to be possible in 10 years.

Engineering: The proposal introduces a completely new way of approaching engineering design of systems that utilize unsteady fluid-structure interaction. This approach will help significantly improve the performance lifting wings and flapping propulsion mechanisms using unsteady fluid dynamics.

5.2 Broader impact: More than 85% of the public school students in the Providence school district belong to low-income households. The lack of availability of high quality resources is a key hurdle in the path of Providence school educators. As part of the CAREER outreach activities, I target this difficulty by building and managing a configurable robotics toolbox. The toolbox is based on commonly available inexpensive (but not affordable for the school children) robotics platforms and therefore, a large amount of documentation for its use is already available. Ensuring the long-term availability of such a resource will enable educational programs using the toolbox to plan for sustained programs over many years, allowing for the interaction with the school students to be tracked from elementary to high school.

The educational and outreach component of the proposal targets the range from elementary school to graduate students. The outreach activity will benefit public school students in the Providence school district by exposing them to robotics. Teaching a core engineering undergraduate course demands an interdisciplinary approach, and the biomechanical inspiration for the course is expected to help recruit and retain women engineers. The mentoring of undergraduate and graduate students in an interdisciplinary environment by inculcating scientific skills is an integral part of this project and my career as an academic.

Prior NSF Support: None.

References

[1] D. R. Warrick, B. W. Tobalske, and D. R. Powers. Aerodynamics of the hovering hummingbird. *Nature*, 435(7045):1094–1097, 2005.

[2] F. E. Fish and G. V. Lauder. Passive and active flow control by swimming fishes and mammals. *Annu. Rev. Fluid Mech.*, 38:193–224, 2006.

[3] F. T. Muijres, L. C. Johansson, R. Barfield, M. Wolf, G. R. Spedding, and A. Hedenström. Leading-edge vortex improves lift in slow-flying bats. *Science*, 319(5867):1250–1253, 2008.

[4] C. P. Ellington, C. Van Den Berg, A. P. Willmott, and A. L. R. Thomas. Leading-edge vortices in insect flight. 1996.

[5] R. B. Srygley and A. L. R. Thomas. Unconventional lift-generating mechanisms in free-flying butterflies. *Nature*, 420(6916):660–664, 2002.

[6] C. P Ellington. The novel aerodynamics of insect flight: applications to micro-air vehicles. *Journal of Experimental Biology*, 202(23):3439–3448, 1999.

[7] S. P. Sane. The aerodynamics of insect flight. *The journal of experimental biology*, 206(23): 4191–4208, 2003.

[8] Z. J. Wang. Dissecting insect flight. *Annu. Rev. Fluid Mech.*, 37:183–210, 2005.

[9] M. S. Triantafyllou, G. S. Triantafyllou, and D. K. P. Yue. Hydrodynamics of fishlike swimming. *Annual review of fluid mechanics*, 32(1):33–53, 2000.

[10] G. V. Lauder, E. J. Anderson, J. Tangorra, and P. G. A. Madden. Fish biorobotics: kinematics and hydrodynamics of self-propulsion. *Journal of Experimental Biology*, 210(16):2767–2780, 2007.

[11] G. Tokić and D. K. P. Yue. Optimal shape and motion of undulatory swimming organisms. *Proceedings of the Royal Society B: Biological Sciences*, 279(1740):3065–3074, 2012.

[12] W. Mm van Rees, M. Gazzola, and P. Koumoutsakos. Optimal shapes for anguilliform swimmers at intermediate Reynolds numbers. *J Fluid Mech*, 722:R3, 2013.

[13] M. Milano and M. Gharib. Uncovering the physics of flapping flat plates with artificial evolution. *Journal of Fluid Mechanics*, 534(1):403–409, 2005.

[14] C. Eloy and L. Schouveiler. Optimisation of two-dimensional undulatory swimming at high Reynolds number. *International Journal of Non-Linear Mechanics*, 46(4):568–576, 2011.

[15] Y. Kawamura, S. Souda, S. Nishimoto, and C. P. Ellington. Clapping-wing micro air vehicle of insect size. In *Bio-mechanisms of Swimming and Flying*, pages 319–330. Springer, 2008.

[16] M. Karpelson, J. P. Whitney, G-Y. Wei, and R. J. Wood. Energetics of flapping-wing robotic insects: Towards autonomous hovering flight. In *Intelligent Robots and Systems (IROS), 2010 IEEE/RSJ International Conference on*, pages 1630–1637. IEEE, 2010.

[17] R. J. Wood. The first takeoff of a biologically inspired at-scale robotic insect. *Robotics, IEEE Transactions on*, 24(2):341–347, 2008.

[18] U. Pesavento and Z. J. Wang. Flapping wing flight can save aerodynamic power compared to steady flight. *Physical review letters*, 103(11):118102, 2009.

[19] J. L. Lions and S. K. Mitter. *Optimal control of systems governed by partial differential equations*, volume 1200. Springer Berlin, 1971.

[20] A. Jameson. Aerodynamic design via control theory. *Journal of Scientific Computing*, 3(3): 233–260, 1988.

[21] A. Jameson, L. Martinelli, and N. A. Pierce. Optimum aerodynamic design using the Navier–Stokes equations. *Theoretical and Computational Fluid Dynamics*, 10(1-4):213–237, 1998.

[22] T. R. Bewley, R. Temam, and M. Ziane. A general framework for robust control in fluid mechanics. *Physica D: Nonlinear Phenomena*, 138(3):360–392, 2000.

[23] J. Kim and T. R. Bewley. A linear systems approach to flow control. *Annu. Rev. Fluid Mech.*, 39:383–417, 2007.

[24] Q. Wang, P. Moin, and G. Iaccarino. Minimal repetition dynamic checkpointing algorithm for unsteady adjoint calculation. *SIAM Journal on Scientific Computing*, 31(4):2549–2567, 2009.

[25] M. Yu, Z. J. Wang, and H. Hu. High-Fidelity Optimization of Flapping Airfoils for Maximum Propulsive Efficiency. *Numerical and experimental investigations on unsteady aerodynamics of flapping wings*, page 129, 2013.

[26] M. Culbreth, Y. Allaneau, and A. Jameson. *High Fidelity Optimization of Flapping Airfoils and Wings*. PhD thesis, Stanford University, 2013.

[27] P. G. Saffman. *Vortex dynamics*. Cambridge university press, 1992.

[28] M. R. Booty and M. Siegel. A hybrid numerical method for interfacial fluid flow with soluble surfactant. *Journal of Computational Physics*, 229(10):3864–3883, 2010.

[29] R. Mittal and G. Iaccarino. Immersed boundary methods. *Annu. Rev. Fluid Mech.*, 37:239–261, 2005.

[30] Top 500 Supercomputer Sites. `www.top500.org/lists/2013/06/`, 2013.

[31] Y. Tanabe and K. Kaneko. Behavior of a falling paper. *Physical review letters*, 73(10):1372–1375, 1994.

[32] L. Mahadevan. Tumbling of a falling card. *Comptes rendus de l'Académie des sciences. Série II, Mécanique, physique, chimie, astronomie*, 323(11):729–736, 1996.

[33] A. Belmonte, H. Eisenberg, and E. Moses. From flutter to tumble: inertial drag and Froude similarity in falling paper. *Physical Review Letters*, 81(2):345, 1998.

[34] L. Mahadevan, W. S. Ryu, and A. D. T. Samuel. Tumbling cards. *Physics of Fluids*, 11(1):1, 1999.

[35] U. Pesavento and Z. J. Wang. Falling paper: Navier-Stokes solutions, model of fluid forces, and center of mass elevation. *Physical review letters*, 93(14):144501, 2004.

[36] A Andersen, U Pesavento, and Z Wang. Unsteady aerodynamics of fluttering and tumbling plates. *Journal of fluid mechanics*, 541:65–90, 2005.

[37] M. H. Hansen, M. Gaunaa, and H. Aagaard Madsen. *A Beddoes-Leishman type dynamic stall model in state-space and indicial formulations*. 2004.

[38] S. L. Brunton and C. W. Rowley. Empirical state-space representations for Theodorsen's lift model. *Journal of Fluids and Structures*, 2013.

[39] T. J. Pedley and S. J. Hill. Large-amplitude undulatory fish swimming: fluid mechanics coupled to internal mechanics. *Journal of Experimental Biology*, 202(23):3431–3438, 1999.

[40] M. A. Jones and M. J. Shelley. Falling cards. *Journal of Fluid Mechanics*, 540:393–425, 2005.

[41] R. K. Shukla and J. D. Eldredge. An inviscid model for vortex shedding from a deforming body. *Theoretical and Computational Fluid Dynamics*, 21(5):343–368, 2007.

[42] K. Singh and T. J. Pedley. The hydrodynamics of flexible-body manoeuvres in swimming fish. *Physica D: Nonlinear Phenomena*, 237(14):2234–2239, 2008.

[43] S. Alben. Simulating the dynamics of flexible bodies and vortex sheets. *Journal of Computational Physics*, 228(7):2587–2603, 2009.

[44] S. Michelin and S. G. L. Smith. An unsteady point vortex method for coupled fluid–solid problems. *Theoretical and Computational Fluid Dynamics*, 23(2):127–153, 2009.

[45] S. Michelin and S. G. L. Smith. Falling cards and flapping flags: understanding fluid–solid interactions using an unsteady point vortex model. *Theoretical and Computational Fluid Dynamics*, 24(1-4):195–200, 2010.

[46] J. X. Sheng, A. Ysasi, D. Kolomenskiy, E. Kanso, M. Nitsche, and K. Schneider. Simulating vortex wakes of flapping plates. In *Natural Locomotion in Fluids and on Surfaces*, pages 255–262. Springer, 2012.

[47] A. J. Chorin. Vortex sheet approximation of boundary layers. *Journal of Computational Physics*, 27(3):428–442, 1978.

[48] A. Leonard. Vortex methods for flow simulation. *Journal of Computational Physics*, 37(3): 289–335, 1980.

[49] J. A. Sethian and A. F. Ghoniem. Validation study of vortex methods. *Journal of Computational Physics*, 74(2):283–317, 1988.

[50] C. R. Anderson. Vorticity boundary conditions and boundary vorticity generation for two-dimensional viscous incompressible flows. *Journal of Computational Physics*, 80(1):72–97, 1989.

[51] A. J. Chorin. Vortex methods. Technical report, Lawrence Berkeley Lab., CA (United States), 1993.

[52] P. Koumoutsakos, A. Leonard, and F. Pepin. Boundary conditions for viscous vortex methods. *Journal of Computational Physics*, 113(1):52–61, 1994.

[53] D. M. Summers and A. J. Chorin. Numerical vorticity creation based on impulse conservation. *Proceedings of the National Academy of Sciences*, 93(5):1881–1885, 1996.

[54] J. D. Eldredge, T. Colonius, and A. Leonard. A vortex particle method for two-dimensional compressible flow. *Journal of Computational Physics*, 179(2):371–399, 2002.

[55] J. Yao and D. S. Stewart. *The dynamics of multi-dimensional detonation*. PhD thesis, Cambridge Univ Press, 1996.

[56] M. Matalon, C. Cui, and J. K. Bechtold. Hydrodynamic theory of premixed flames: effects of stoichiometry, variable transport coefficients and arbitrary reaction orders. *Journal of Fluid Mechanics*, 487:179–210, 2003.

[57] M. Bar-Lev and H. T. Yang. Initial flow field over an impulsively started circular cylinder. *Journal of Fluid Mechanics*, 72(04):625–647, 1975.

[58] P. Koumoutsakos and A. Leonard. High-resolution simulations of the flow around an impulsively started cylinder using vortex methods. *Journal of Fluid Mechanics*, 296(1):1–38, 1995.

[59] L. Greengard and V. Rokhlin. A fast algorithm for particle simulations. *Journal of computational physics*, 73(2):325–348, 1987.

[60] R. Yokota and L. Barba. Hierarchical N-body simulations with autotuning for heterogeneous systems. *Computing in Science & Engineering*, 14(3):30–39, 2012.

[61] I. J. Sobey. *Introduction to interactive boundary layer theory*, volume 3. Oxford University Press, 2000.

[62] S. Mandre, M. Mani, and M. P. Brenner. Precursors to Splashing of Liquid Droplets on a Solid Surface. *Phys. Rev. Lett.*, 102(13):134502, 2009.

[63] S. Mandre and M. P. Brenner. The mechanism of a splash on a dry solid surface. *Journal of Fluid Mechanics*, 690:148, 2012.

[64] M. Mani, S. Mandre, and M. P. Brenner. Events before droplet splashing on a solid surface. *J. Fluid Mech.*, 647:163–185, 2010.

[65] T. M. Schneider, S. Mandre, and M. P. Brenner. Algorithm for a microfluidic assembly line. *Physical Review Letters*, 106(9):094503, 2011.

[66] Z. Wei, S. Mandre, and L. Mahadevan. The branch with the furthest reach. *EPL (Europhysics Letters)*, 97:14005, 2012.

[67] S. Mandre and L. Mahadevan. A generalized theory of viscous and inviscid flutter. *Proceedings of the Royal Society A: Mathematical, Physical and Engineering Science*, 466(2113):141–156, 2010.

[68] A. He, K. Nguyen, and S. Mandre. Capillary interactions between nearby interfacial objects. *EPL (Europhysics Letters)*, 102(3):38001, 2013.

[69] W. Noll. The Role of the Professor. `http://repository.cmu.edu/math/13`, 1997.

[70] D. Lentink, U. K. Müller, E. J. Stamhuis, R. De Kat, W. Van Gestel, L. L. M. Veldhuis, P. Henningsson, A. Hedenström, J. J. Videler, and J. L. Van Leeuwen. How swifts control their glide performance with morphing wings. *Nature*, 446(7139):1082–1085, 2007.

[71] N. J. Balmforth, S. A. Ghadge, A. Kettapun, and S. D. Mandre. Bounds on double-diffusive convection. *Journal of Fluid Mechanics*, 569(1):29–50, 2006.

[72] K. Ip and S. Mandre. Enhanced evaporation from surfaces of width comparable to that of the mass boundary layer thickness. *Bulletin of the American Physical Society*, 56, 2011.

[73] K. Nguyen, M. Miller, and S. Mandre. Fluid Surface Deformation by Objects in the Cheerios Effect. *Bulletin of the American Physical Society*, 57, 2012.

[74] 2012 Rhode Island Kids Count Factbook. Rhode Island KIDS COUNT, Providence, RI, 2012.

[75] L. E. Carlson and J. F Sullivan. Hands-on engineering: learning by doing in the integrated teaching and learning program. *International Journal of Engineering Education*, 15:20–31, 1999.

[76] A. T. Jeffers, A. G. Safferman, and S. I. Safferman. Understanding K-12 engineering outreach programs. *Journal of professional issues in engineering education and practice*, 130(2):95–108, 2004.

[77] S. Brophy, S. Klein, M. Portsmore, and C. Rogers. Advancing engineering education in P-12 classrooms. *Journal of Engineering Education*, 97(3):369–387, 2008.

[78] E. Cejka, C. Rogers, and M. Portsmore. Kindergarten robotics: Using robotics to motivate math, science, and engineering literacy in elementary school. *International Journal of Engineering Education*, 22(4):711–722, 2006.

[79] X. Yu and J. B. Weinberg. From the guest editors-Robotics in education: new platforms and environments. *Robotics & Automation Magazine, IEEE*, 10(3):3–3, 2003.

[80] S. Galvan, D. Botturi, A. Castellani, and P. Fiorini. Innovative robotics teaching using lego sets. In *Robotics and Automation, 2006. ICRA 2006. Proceedings 2006 IEEE International Conference on*, pages 721–726. IEEE, 2006.

[81] M. R. Blanchard, S. A. Southerland, and E. M. Granger. No silver bullet for inquiry: Making sense of teacher change following an inquiry-based research experience for teachers. *Science Education*, 93(2):322–360, 2009.

[82] C. T. Melear, J. D. Goodlaxson, T. R. Warne, and L. G. Hickok. Teaching preservice science teachers how to do science: Responses to the research experience. *Journal of Science Teacher Education*, 11(1):77–90, 2000.

[83] Washington DC. American Association for the Advancement of Science. *Benchmarks for science literacy*. ERIC Clearinghouse, 1993.

[84] S. Olson and S. Loucks-Horsley. *Inquiry and the National Science Education Standards: A guide for teaching and learning*. National Academies Press, 2000.

[85] M. J. Lighthill. A new method of two-dimensional aerodynamics design. In *R&M1111, Aeronautical Research Council*. Citeseer, 1945.

Data Management Plan

Sharing of Primary Data Sharing of primary data, overseen by the PI, will be implemented through (a) dissemination via peer-reviewed publication, conference proceedings including oral presentations, and (b) through the Brown University Digital Repository for academic researchers and educators who would like to use it in for education or research.

Expected data, data formats and dissemination The types of data produced within this proposal includes theoretical models, computational programs and solutions, and digital flow visualization. The most important anticipated results are a zoology of optimal actuation strokes that maximize propulsive force. All of this data will be stored in non-proprietary .txt, .dat, or .m files. The provision for publishing online supplementary material will also be used extensively to archive and disseminate results.

Any significant raw data not suitable for publishing as Supplementary Information, especially contained in large files, that forms the basis of the scientific conclusions drawn in the publications, or that represents high-resolution datasets unsuitable for archival in scientific journals, will be disseminated using Brown University's Digital Repository maintained by the university's library. The university provides a space of 4 GB to all its academic patrons, and has provision for more space if required. Upon request, any requested data generated as part of this research will also be shared with scholars in the field through the Digital Repository.

Period of data retention The data retention length of research data will be five years after conclusion of the award or five years after public release, whichever is later. Public release of data will be immediately after publication, and submission for publication is planned to be timely. The Brown Digital Repository plans to archive the data indefinitely.

Data storage and preservation of access The primary storage facility of the data generated in this proposal will be on a hard drive on a designated computer in the PI's laboratory. While the designated graduate student will keep copies on his or her personal computer all files belonging to this project will be kept on a central computer, which will be constantly backed up. This computer will be accessible to both the PI and the graduate student trained for the project and hence will make for an efficient and effective storage solution. More shared data storage is available through the Brown universities Center for Computing and Visualization.

Facilities

Many computations proposed in this project are rapid enough that they can be carried on a desktop or a personal computer. The later sections of the proposal require high-performance computing; the PI has access to a High Performance Computing facility maintained by Brown University's Center for Computation and Visualization.

The PI has access to a laboratory to construct the robotic swimmers for the outreach activity.

Budget justification

Personnel The main expense in the budget is for supporting a graduate student. The theoretical and numerical calculations proposed for this project are advanced, and suitable only for a graduate student. Faculty salary of 0.25 months is included commensurate with the enlisted effort. Fringe benefits are calculated at the rates of 30.5% (eff. 7/1/13) increasing to 31% 7/1/14.

Facilities and research supplies We also need high performance computing for the many solutions of partial differential equations; such a computing facility is available locally at marginal cost through the Brown Center for Computation and Visualization (listed as CCV in the budget). Supplies for outreach activities are also included in the budget.

Travel In accordance with the mentoring plan, the budget includes expenses for travels to conferences.

Administrative costs A federally negotiated rate of 62.5% is used to calculate the administrative and other indirect costs. Health fees are excluded from the base value used for calculating the indirect costs.